

# Rod Photoreceptor Function in Children With Mitochondrial Disorders

Linda L. Cooper, MD; Ronald M. Hansen, PhD; Basil T. Darras, MD; Mark Korson, MD; Frances E. Dougherty, MD, PhD; John M. Shoffner, MD; Anne B. Fulton, MD

**Objective:** To test the hypothesis that function of the rod photoreceptors is abnormal in pediatric patients with mitochondrial disorders.

**Methods:** Patients (n=22; median age, 5 years) with a deficiency of 1 or more of the mitochondrial enzyme complexes, or a mutation in mitochondrial DNA, were studied by means of scotopic, full-field electroretinography (ERG). The conditions of ERG testing allowed derivation of the parameters of the activation of rod phototransduction from the ERG a-wave, and postreceptoral function from b-wave and P<sub>2</sub> stimulus-response functions. The deactivation of phototransduction was studied in 5 patients. The patients' ERG responses were compared with those of healthy control subjects (n=25).

**Results:** Responses from 19 patients were sufficient for

analysis of rod photoreceptor and postreceptoral function. Saturated amplitudes of the rod photoreponse and b-wave sensitivity were significantly depressed in the patients. Saturated amplitudes of rod cell and P<sub>2</sub> responses were correlated. The kinetics of deactivation of phototransduction were slowed even if the kinetics of activation were normal.

**Conclusions:** In patients with mitochondrial disorders, some abnormalities of the scotopic ERG responses originate in the rod photoreceptors, but postreceptoral processes may also be abnormal. From a practical perspective, ERG testing can contribute to diagnosis of mitochondrial disorders.

*Arch Ophthalmol.* 2002;120:1055-1062

From the Departments of Ophthalmology (Drs Cooper, Hansen, and Fulton) and Neurology (Dr Darras), Children's Hospital Boston and Harvard Medical School, Boston, Mass; Division of Metabolism, Department of Pediatrics, Floating Hospital for Children, Tufts New England Medical Center, Boston (Dr Korson); and Horizon Molecular Medicine, Norcross, Ga (Drs Dougherty and Shoffner). Dr Cooper is now with Ivey Institute of Ophthalmology, London, Ontario.

**N**EARLY ALL of the energy storage molecule adenosine triphosphate (ATP) is produced by oxidative phosphorylation (OXPHOS).<sup>1,2</sup> Although all cells need ATP, some cells, such as the photoreceptors, have very high requirements for ATP production.<sup>3</sup> The OXPHOS pathway involves 5 intramitochondrial enzyme complexes (I to V) whose subunits are encoded by nuclear DNA plus mitochondrial DNA (mtDNA) genes. The genetic complexity of this enzyme system produces a wide variety of multisystem or tissue-specific diseases with mendelian inheritance patterns, maternal inheritance of mtDNA mutations, or the sporadic occurrence of mutations in either genome. Because mitochondrial disease tends to produce clinical abnormalities in cells with high energy requirements and low replicative potentials, photoreceptors are predicted to show defects in patients harboring OXPHOS defects.

The photoreceptors are some of the most highly ATP-dependent cells in the body.<sup>3,4</sup> Rods use tremendous amounts of energy to support the ionic pumps that keep the cell in a response-ready state,<sup>5</sup> turn over

outer segment discs,<sup>6</sup> and power phototransduction processes.<sup>7</sup> The photoreceptor's inner segments are packed with mitochondria<sup>8</sup>; 90% of the retina's mitochondria are in the inner segments.<sup>9</sup> Thus, dysfunction of the rod photoreceptors is predicted in patients with mitochondrial disorders. Indeed, retinal degeneration is a recognized feature of some mitochondrial disorders, such as Kearns-Sayre syndrome.<sup>10-12</sup> Patients with other types of mitochondrial disorders are considered at risk for retinal involvement.<sup>1,10,11,13-15</sup>

The retina is accessible for study of molecular processes in the rod photoreceptors by means of contemporary electroretinographic (ERG) procedures. Herein, we tested the hypothesis that rod cell function is abnormal in pediatric patients with mitochondrial disorders. Specifically, the activation and deactivation of rod photoreceptor responses were studied.

## RESULTS

Sample a- and b-wave results from 4½-year-old patient 22 are shown in **Figure 1**. Nineteen of the 22 patients had sufficient response amplitudes for rod photore-

## SUBJECTS AND METHODS

The 22 patients are grouped according to type of mitochondrial disorder in **Table 1**. For inclusion in this study, each patient was required to have deficiencies of 1 or more enzyme complexes in mitochondria isolated from fresh muscle, or mutation of mtDNA. Twenty had deficiencies in 1 or more of the mitochondrial enzyme complexes (Table 1). To date, no mutation of mitochondrial or nuclear DNA has been identified in any of these 20 patients. A large deletion in mtDNA common in Kearns-Sayre syndrome was found in patient 1. An mtDNA point mutation (T8993G) in ATPase 6 was detected in patient 2. Abnormalities in other biochemical measures and clinical features consistent with a mitochondrial disorder were not sufficient for inclusion.

All patients had abnormal systemic features (Table 1). Patients 1, 2, 12, and 15 through 19 had ophthalmoscopic evidence of retinal degeneration. Patients 12, 15, and 16 initially had been seen in infancy with visual impairment, marked attenuation of ERG responses, and neurologic abnormalities (Table 1) and, thus, had a clinical diagnosis of complicated<sup>16</sup> Leber congenital amaurosis, or congenital retinal blindness. Patients 3 and 10 had optic atrophy without other ophthalmoscopic signs of retinal degeneration; mutations of mtDNA associated with Leber optic atrophy have not been identified in these patients. All others had normal fundi on ophthalmoscopy. Except for patient 1 with Kearns-Sayre syndrome, none had ptosis or ophthalmoplegia. Informed consent for the muscle biopsy and ERG was obtained from the parents.

### MEASUREMENTS OF MITOCHONDRIAL ENZYME COMPLEXES

For the studies of OXPHOS enzyme activities, a quadriceps muscle biopsy was performed while the patient was under general anesthesia. Mitochondria were immediately isolated from the skeletal muscle and OXPHOS enzyme activities were measured as previously described.<sup>1,17,18</sup> Abnormal OXPHOS specific activity was defined as a value below the 5% confidence level calculated from OXPHOS values measured in muscle biopsy specimens obtained from 40 healthy control subjects, aged 18 to 49 years, with no family history of the mitochondrial spectrum of diseases; normal results of neurologic examination performed by one of us (J.M.S.); normal levels of organic acids, amino acids, and blood carnitine; and normal muscle structure on light and electron microscopy. The

controls did not include infants and children because of the invasive nature of the muscle biopsy. To obtain OXPHOS enzyme data from children free of OXPHOS disease, one author's (J. M. S.) clinical database of patients referred for OXPHOS testing was reviewed. The OXPHOS enzyme levels of 44 children, aged 4 months to 10½ years (median, 5½ years), whose final diagnoses were other than OXPHOS disease did not differ significantly from those of the adult control group. Therefore, for OXPHOS diagnosis in the children, values were compared with those for the 18- to 49-year-old controls.

### ERG PROCEDURES

The median age at ERG testing was 5 years (range, 3 months to 16 years). The pupils were dilated with 1% cyclopentolate hydrochloride, and the subject was dark adapted for 30 minutes. Eight patients had ERG testing while under anesthesia (Table 1) for multidisciplinary evaluations. For these, dark adaptation was accomplished with light-tight eye patches.<sup>19</sup> After dark adaptation, in dim red light, 0.5% proparacaine hydrochloride was instilled and Burian-Allen bipolar electrodes were placed on the corneas. A ground electrode was placed on the skin over the mastoid.

Blue (Wratten 47B,  $\lambda < 510$  nm; Eastman Kodak Co, Rochester, NY) strobe stimuli (Novatron of Dallas, Dallas, Tex) were delivered through a 41-cm integrating sphere, were controlled in intensity by calibrated, neutral-density filters, and ranged from those evoking a small ( $< 15$ - $\mu$ V) b-wave to those that saturated the a-wave amplitude in controls.<sup>20</sup> The unattenuated flash, measured with a detector (S350; UDT Instruments, Baltimore, Md) placed at the position of the subject's cornea, was 3.82 log  $\mu$ W/cm<sup>2</sup> per flash. The scotopic troland value of the stimulus was calculated by taking each subject's pupillary diameter into account.<sup>20</sup>

All responses were differentially amplified (alternating current coupled 1 to 1000 Hz; 1000 gain), displayed on an oscilloscope, and stored on a disk for analysis (Compact 4; Nicolet Biomedical Inc, Madison, Wis). An adjustable voltage window was used to reject records contaminated by artifacts. Two to 16 responses were averaged in each stimulus condition. The interstimulus interval ranged from 2 to 60 seconds.

### Activation of Phototransduction in Rods

Rod photoresponse characteristics were estimated by means of the Hood and Birch<sup>21</sup> formulation of the Lamb and Pugh<sup>7,22</sup>

response parameters  $R_{mp3}$  and  $S$  to be calculated from the a-waves, and log  $\sigma$  and  $V_{max}$  to be calculated from the b-waves. Of these parameters, all except  $S$  differed significantly between the patients and controls (Table 2). In 3 (patients 12, 15, and 16), these analyses could not be done because the maximum a- and b-wave amplitudes were 30  $\mu$ V or less. One of these 3 (patient 15) was the youngest studied, aged 3 months. At age 3 months, normal ERG responses are readily detectable with all response parameters described herein being calculable.<sup>20</sup> For the 19 patients,  $S$ ,  $R_{mp3}$ , log  $\sigma$ , and  $V_{max}$  did not vary significantly with age. The responses of those tested un-

der anesthesia (Table 1) did not differ from those tested awake.

In the 19 patients,  $R_{mp3}$ , log  $\sigma$ , and  $V_{max}$  were broadly distributed, with almost all values being below the normal mean (**Figure 2**). The distribution of the patients' values of  $S$  was similar to normal. If, as may be done for clinical decision making, the lower limit of the 95% prediction interval defined normal, 14 (74%) of the 19 patients had abnormal log  $\sigma$ , 9 (47%) had abnormal  $R_{mp3}$ , 7 (37%) had abnormal  $V_{max}$ , and 2 (11%) had abnormal  $S$ .

A diagram of  $P_2$ , obtained by subtraction of the rod photoresponse (equation 1) from the intact ERG,<sup>32,33</sup> and

model of the biochemical processes involved in the activation of rod phototransduction. The main parameters of this model are  $S$  and  $R_{mp3}$  ( $S$  is a sensitivity parameter, and  $R_{mp3}$  is the amplitude of the saturated rod response<sup>21</sup>). A curve-fitting routine (MATLAB, *fmins* subroutine; The MathWorks, Inc, Natick, Mass) was used to determine the best-fitting values of  $S$ ,  $R_{mp3}$ , and  $t_d$ , a brief delay, in the following equation:

$$(1) \quad R(I,t) = \{1 - \exp[-0.5 I S (t - t_d)^2]\} R_{mp3}$$

In this equation,  $I$  is the flash in estimated number of isomerizations per rod per flash. Approximately 8.5 isomerizations per rod per flash are produced by 1 scotopic troland second.<sup>23</sup> Fitting of the model was restricted to the leading edge of the a-wave response, or to a maximum of 20 milliseconds after stimulus onset. All 3 parameters were free to vary. For controls,<sup>20</sup> the mean value of  $S$  is 10.19 sec<sup>-2</sup> (SD, 1.6 sec<sup>-2</sup>) and that of  $R_{mp3}$  is 385  $\mu$ V (SD, 75  $\mu$ V).

#### Deactivation of Phototransduction in Rods

The recovery of the rod cell's response to light was evaluated by means of a paired flash paradigm<sup>24</sup> in patients 2, 5, 8, 21, and 22 who, during the ERG procedure, were recognized to have robust retinal responses. Paired flash paradigms have been used to study the deactivation of phototransduction in normal rods and in patients with retinal diseases.<sup>25-28</sup> At 7 selected interstimulus intervals (2 to 120 seconds) after a test flash, a probe flash was presented. Between each test-probe pair, 2 minutes in the dark was allowed. The amplitude of the response to the probe was expressed as a percentage of amplitude of the response to the test flash alone. For controls ( $n=8$ ), amplitude is 50% when the median interstimulus interval is 3 seconds (range, 2-5 seconds) and 100% at the 120-second interstimulus interval.

#### Analysis of B-Waves

In addition to the rod photoresponse, the b-waves in the patients' ERG records were analyzed. The b-wave stimulus-response function

$$(2) \quad V/V_{max} = I/(I + \sigma)$$

was fit to the b-wave amplitudes of each subject by means of an iterative procedure that minimized the mean square deviation of the data from the equation.<sup>20</sup> In this equation,  $V$  was the b-wave amplitude produced by flash intensity  $I$ , and  $V_{max}$ , the saturated b-wave amplitude.

The flash intensity that evokes a half-maximum response amplitude is  $\sigma$ . Thus,  $\sigma$  is the semisaturation constant, and  $1/\sigma$  is a measure of sensitivity. The stimulus-response function was fit up to those higher intensities at which a-wave intrusion occurs.<sup>29</sup> For controls,<sup>20</sup> the mean value of  $\log \sigma$  is  $-0.88$  log scotopic troland seconds (SD, 0.10 log scotopic troland seconds) and that of  $V_{max}$  is 379  $\mu$ V (SD, 59  $\mu$ V) (**Table 2**). A scotopic stimulus frequently used in clinical testing, blue 8 (equivalent to approximately  $+0.9$  log scotopic troland second) is included in the stimulus-response test. For controls ( $n=25$ ), the mean amplitude of the b-wave response to blue 8 is 453  $\mu$ V (SD, 116  $\mu$ V).

#### Analysis of $P_2$

In an analysis reminiscent of that of Granit,<sup>30,31</sup> the ERG waveform is considered to be the sum of the photoreceptor and postreceptor retinal responses.<sup>32,33</sup> Equation 1 modeled the rod photoresponse, sometimes called  $P_3$ . The photoresponse was digitally subtracted from the ERG waveform to obtain  $P_2$ , which is thought to represent mainly the on-bipolar cell response, but also activity in other second- and third-order retinal neurons.<sup>32-38</sup> In an analysis similar to that using equation 2 for the b-wave, the  $P_2$  stimulus-response function was fit with

$$(3) \quad P_2/P_{2max} = I/(I + k_{p2}),$$

where  $P_{2max}$  is the saturated amplitude and  $k_{p2}$  is the semisaturation constant.

The on-bipolar cells have their own G-protein cascade. To evaluate the kinetics of the G-protein cascade,<sup>37,38</sup> the latency at which  $P_2$  reached 50  $\mu$ V was noted. In normal retina, this latency, plotted as a function of stimulus intensity on log-log coordinates, is a linear function<sup>37</sup> with slope of about  $-0.2$ . For our 25 controls,<sup>20</sup> the mean slope was  $-0.21$  (SD, 0.05). Departures from this relationship have been taken as indicative of dysfunction of the on-bipolar cells' G-protein cascade.<sup>37</sup>

#### STATISTICAL ANALYSIS

Although for clinical purposes both eyes were tested, for analysis, data from the left eye were selected. The patients' and controls' ERG parameters were compared (*t* test). In addition, individual patients' results were compared with the prediction interval for controls.<sup>20</sup> The prediction interval gives the range of values within which results from individuals in the healthy population are expected to fall.<sup>39</sup>

sample  $P_2$  records are shown in **Figure 3**. The parameters of the  $P_2$  stimulus-response function,  $P_{2max}$  and  $\log k_{p2}$ , calculated by the fit of equation 3 to the  $P_2$  stimulus-response data, differed significantly between the patients and controls (Table 2). In Figure 3C, the  $\log P_2$  latency function for patient 21 is shown. This latency function, obtainable in 19 patients, had the slopes summarized in Figure 3D. The normal slopes in the patients suggested that in the bipolar cells, the G-protein cascade<sup>37</sup> was not disturbed. The low rod photoreceptor response amplitude was significantly correlated with low  $P_2$  amplitude; the departures of  $P_{2max}$  and  $R_{mp3}$  from nor-

mal (**Figure 4**) were significantly correlated (slope, 1.10;  $\chi^2=0.80$ ;  $P<.01$ ).

Results of the paired flash test in the 5 patients (patients 2, 5, 8, 21, and 22) are summarized in **Figure 5**. Of note, the activation of rod phototransduction was normal in all of these children except patient 2; each had values of  $S$  and  $R_{mp3}$  within the 95% prediction interval for normal. With decreasing time after the test flash, as the sample records for patient 8 illustrate (Figure 5A), the amplitude of the response to the probe flash decreased in patients and controls. The interstimulus interval (Figure 5B) at which the response was 50%

**Table 1. Clinical Characteristics of Patients**

Mitochondrial Disorder	Patient No./Age/Sex	Ophthalmic Diagnoses	Systemic Features
Kearns-Sayre syndrome	1/10 y 8 mo/F	Ptosis; ophthalmoplegia; pigmentary retinopathy	Cardiomyopathy; hearing impaired
Leigh disease	2*/3 y 3 mo/F	Pigmentary retinopathy	Hypotonia; developmental delay
Complex I	3/9 y 9 mo/F	Optic atrophy; rotary nystagmus	Hearing impairment; developmental delay; intention tremor
	4/7 y 3 mo/M	Photophobia; otherwise normal eyes	Seizures; ataxia; delayed motor development
	5*/5 y 5 mo/F	Exotropia; myopia; low vision	Global developmental delay; hypotonia; scoliosis
	6*/9 y 5 mo/M	Astigmatism, 4 diopters	Attention-deficit/hyperactivity disorder
	7*/6 y 4 mo/M	Normal eyes	Autistic features; seizure disorder
	8*/6 y 8 mo/M	Normal eyes	Motor and cognitive delays; hypotonia; hearing impairment
Complexes I and III	9/4 y 3 mo/M	Low vision; normal eyes	Seizure disorder; developmental delays
	10/16 y 6 mo/M	Optic atrophy	Dystonia
	11*/2 y 8 mo/F	Ptosis; jaw winking	Episodic hypertension; autonomic instability; language delays
Complexes I and IV	12/7 y 2 mo/F	Congenital retinal blindness	Global developmental delays
	13/8 mo/M	Esotropia; hyperopia	Dystonia
	14/1 y 6 mo/F	Normal eyes	Developmental delay; hypotonia
	15†/3 mo/M	Congenital retinal blindness	Seizure disorder; global developmental delays
	16†/2 y 9 mo/F	Congenital retinal blindness; nystagmus	Facial tic
	17†/6 y 1 mo/F	Early pigmentary retinopathy	Ataxia
	18†/10 y 4 mo/F	Pigmentary retinopathy	Ataxia; dysmetria
	19†/10 y 4 mo/F	Pigmentary retinopathy	Polyneuropathy, sensory > motor
Multiple complex deficiencies	20/1 y 1 mo/M	Nystagmus	Hypotonia
	21*/2 y 4 mo/M	Ocular motor apraxia	Developmental delay; renal tubular acidosis; hypotonia
	22*/4 y 6 mo/M	Normal eyes	Autism

\*Electroretinographic testing was done with the patient under anesthesia.

†Patients 15 and 16 are siblings; patients 17, 18, and 19 are siblings.

**Table 2. Comparison of Responses in Patients and Control Subjects\***

Electroretinogram Parameter	Mean (SD)		t	P Value
	Patients (n = 19)	Control Subjects (n = 25)		
$R_{mp3}$ , $\mu V$	282 (103)	385 (75)	3.87	<.001
S, $s^{-2}$	9.52 (2.2)	10.2 (1.60)	-1.04	.30
Log $\sigma$ , scotopic troland seconds	-0.41 (0.47)	-0.88 (0.11)	4.81	<.001
$V_{max}$ , $\mu V$	283 (121)	377 (58)	-3.48	.001
Log $k_{p2}$ , scotopic troland seconds	-0.32 (0.43)	-0.84 (0.13)	5.51	<.001
$P_{2max}$ , $\mu V$	403 (176)	660 (110)	-5.94	<.001

\* $R_{mp3}$  indicates the amplitude of the saturated rod response; S, a sensitivity parameter; log  $\sigma$ , logarithm of the semisaturation constant;  $V_{max}$ , the saturated b-wave amplitude; log  $k_{p2}$ , semisaturation constant; and  $P_{2max}$ , the saturated P<sub>2</sub> amplitude.

of the dark-adapted response amplitude was more than twice as long in the patients (patient 2, 8 seconds; patients 5 and 22, 10 seconds; patient 8, 12 seconds; and patient 21, 9 seconds) as in any of the controls (n=8; range, 2-5 seconds; median, 3 seconds). Thus, the recovery of the rod cell's response, which depends on recovery of the circulating current,<sup>5,7,22</sup> was delayed in the patients.

The ERG parameters S,  $R_{mp3}$ , log  $\sigma$ , and  $V_{max}$  were all normal in only 5 patients. Two of these, patients 3 and 10, had optic atrophy as the predominant ophthalmic abnormality. The other 3, patients 9, 11, and 20, were among the youngest studied.

**COMMENT**

The scotopic ERG data presented herein provide evidence of abnormal rod photoreceptor function in pediatric patients with mitochondrial disorders. Significant deficits (Table 2) in  $R_{mp3}$ , the saturated amplitude of the rod cell response, and significant delays in the recovery of the photoresponse (Figure 5) were found. In these patients, low  $R_{mp3}$  may not be due to a low number of channels in the photoreceptor cell but to insufficient energy for the photoreceptors' ionic pumps. The sodium pumps require enormous amounts of energy.<sup>5</sup> Although the normal kinetics of P<sub>2</sub> (Figure 3D) are evidence that function of the G-protein cascade in the on-bipolar cells is normal, the data do not rule out dysfunction at the photoreceptor-bipolar synapse, or intrinsic to the second- and third-order neurons. Such dysfunction could be the basis for the observed b-wave abnormalities. Deficits in b-wave sensitivity, log  $\sigma$ , occurred more frequently than in any other a-wave or b-wave response parameter.

The sensitivity parameter for the rod photoreceptor response, S, was relatively spared (Table 2 and Figure 2). Up-regulation of the anaerobic pathway protects rod cell sensitivity from experimental blockade of mitochondrial function.<sup>40</sup> Possibly in the patients with mitochondrial disorders the anaerobic system protects rod cell sensitivity until photoreceptor disease is advanced. Normal values of S are consistent with normal content of rhodopsin and normal rod outer segment lengths.

Tissues (such as the retina) and organs (such as the brain) with high requirements for ATP show abnormalities in these patients with mitochondrial disorders. Sei-

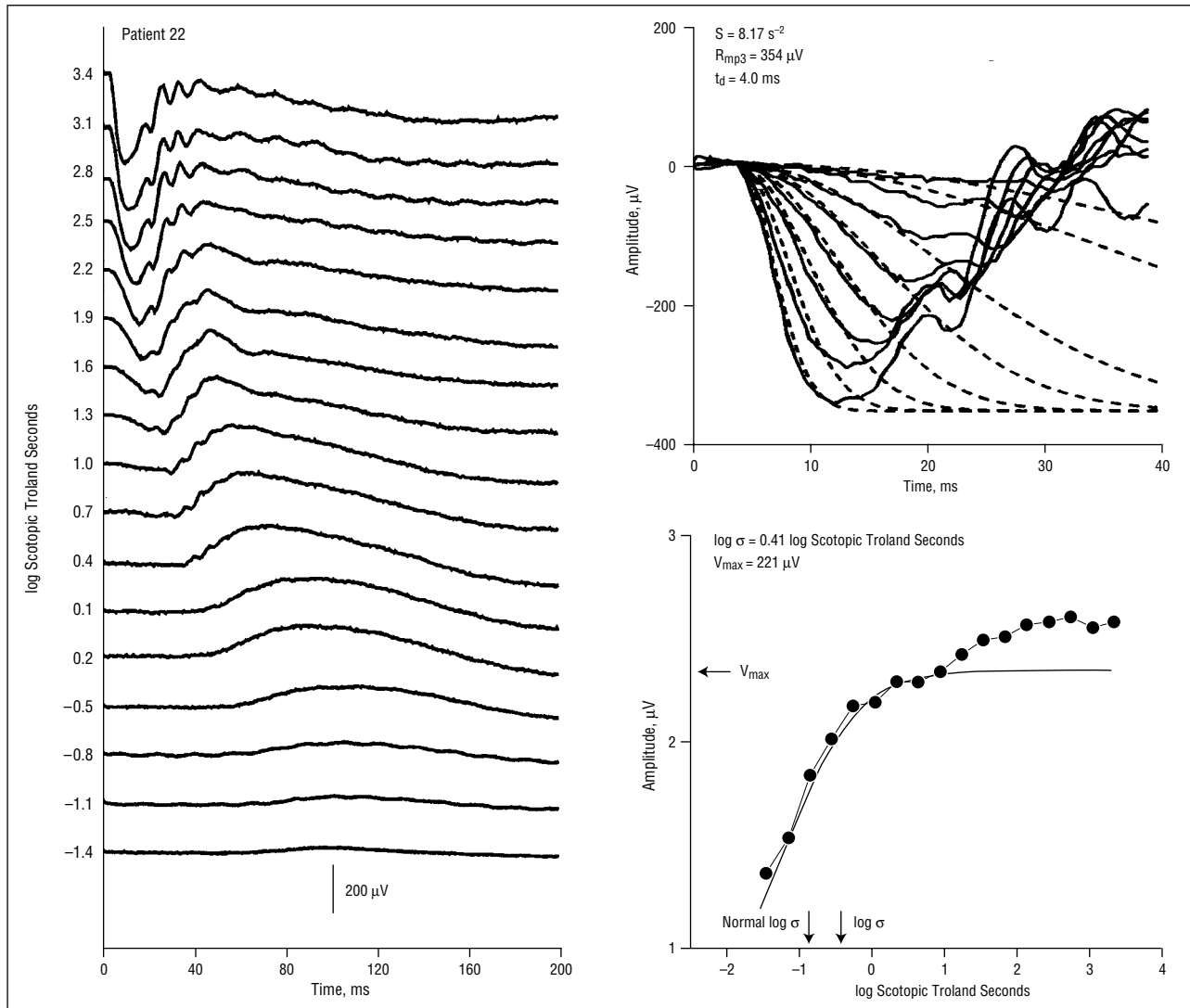


**Figure 1.** Sample records from 4½-year-old patient 22 and model fits to the a-wave (equation 1) and b-wave (equation 2) data.

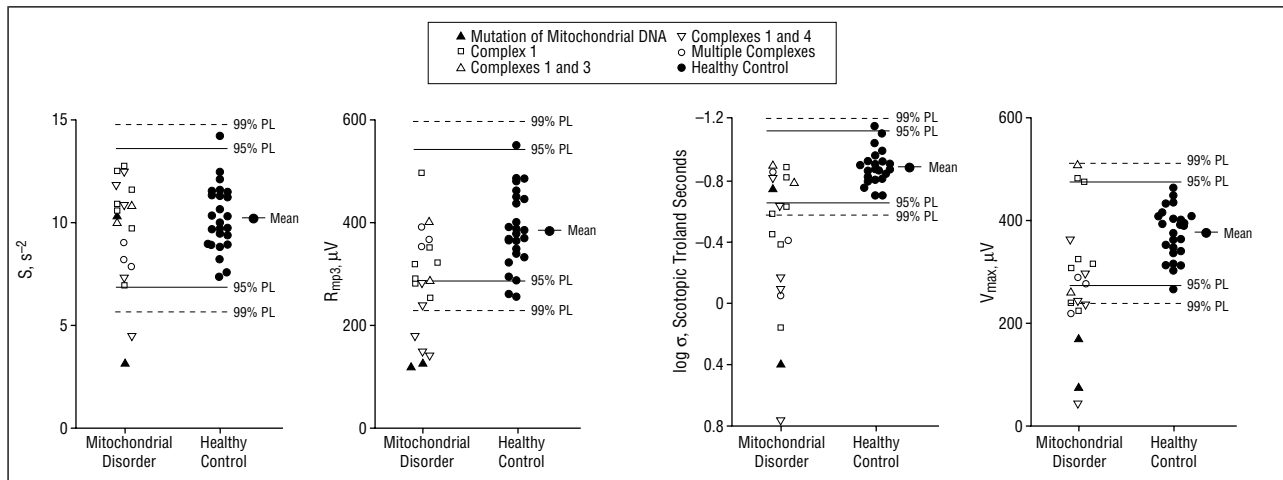


**Figure 2.** Rod photoreponse parameters,  $S$  and  $R_{mp3}$ , and b-wave parameters,  $\log \sigma$  and  $V_{max}$ , in patients ( $n=19$ ) and healthy control subjects ( $n=25$ ). The upper and lower limits of the 95th and 99th prediction intervals and the normal means are as indicated.

zures, developmental delays, and hypotonia, which were common in our patients (Table 1), are evidence of central nervous system and neuromuscular involvement. The

combination of such systemic abnormalities and ocular involvement, as evidenced by significant ERG deficits, should prompt more detailed laboratory evaluations for

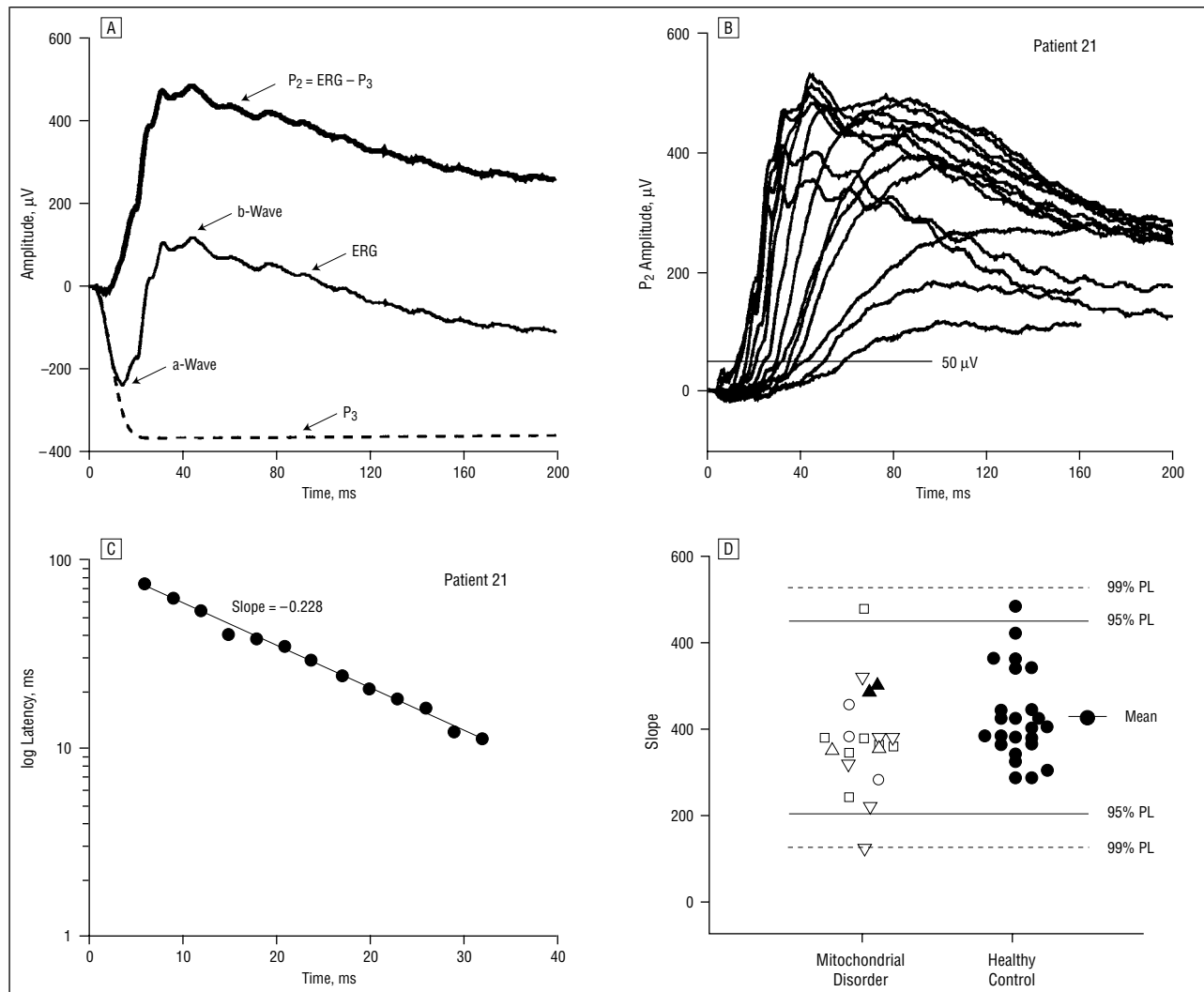


**Figure 3.** Summary  $P_2$  analysis and results. A, Subtraction of the rod photoresponse (labeled  $P_3$ ) from the intact electroretinogram (ERG) waveform yields the  $P_2$  response. B, The family of  $P_2$  waves for patient 21 is shown with the 50- $\mu$ V level marked. C, Log latency, at 50  $\mu$ V, is plotted as a function of log stimulus intensity. D, The slopes of the  $P_2$  latency functions in the patients and control subjects are compared.

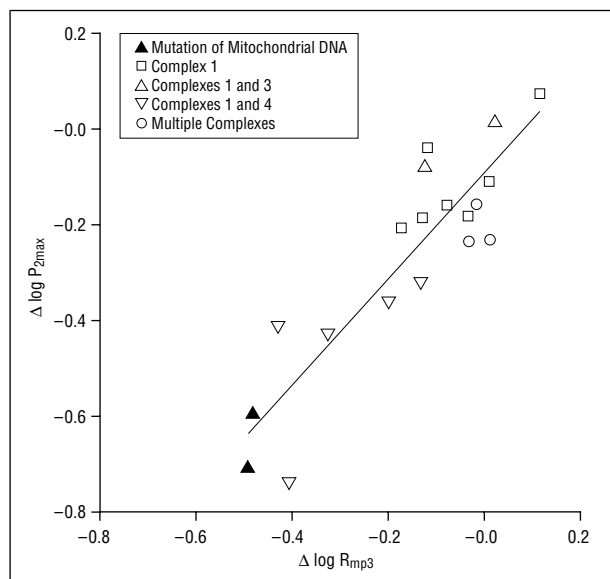


**Figure 4.** The departures of saturated amplitude of the rod photoreceptor response ( $R_{mp3}$ ) and the on-bipolar cell response ( $P_{2max}$ ) from normal shown on a log-log plot.

mitochondrial disease. As a rule of thumb, mitochondrial diseases can be suspected clinically if 2 or more such organs are affected.<sup>1</sup> Identification of a mitochondrial disorder can be critical to the child's general health, as vital organs, including not only the brain but also the heart and kidneys, may become diseased in mitochondrial disorders. Diagnosis of a mitochondrial disorder is also important for evaluation of risk of recurrence of disease in the family.

The majority of these patients (17 of 22 [77%]) had some statistically significant abnormality (below the 95% prediction interval) of the rod-mediated ERG responses. Thus, ERG, a noninvasive test, may help identify patients with mitochondrial disorders. For clinical detection of the retinal dysfunction in a patient with suspected mitochondrial disorder, one might study the ERG b-wave that can be obtained with stimuli delivered by widely available equipment. The most frequent abnormality (Figure 2) was in a b-wave parameter,  $\log \sigma$ . The b-wave semisaturation constant is calculated by taking into account many responses to a range of stimulus intensities. The amplitude of b-wave responses to selected stimuli, such as blue 8,

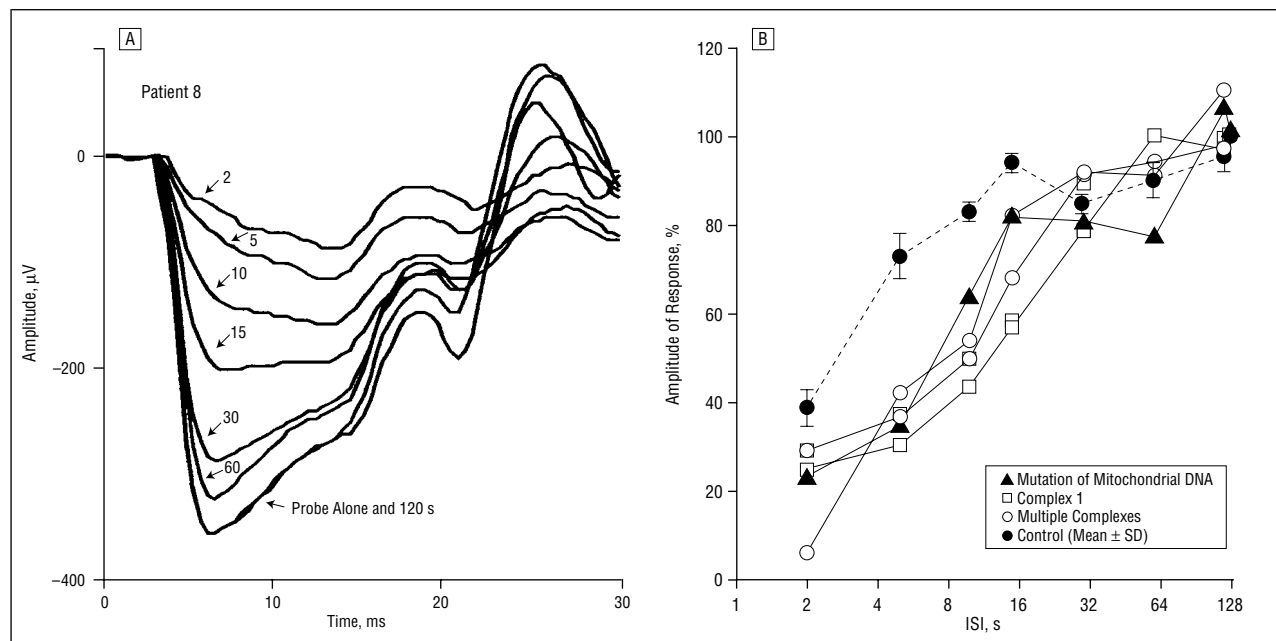


**Figure 5.** Results of the paired flash test. A, The a-wave responses of patient 8 to the test and probe flashes at indicated interstimulus intervals. B, The patients' (n=5) results compared with the mean responses of normal control subjects (n=8). The interstimulus interval at which the response to the probe flash was 50% of the amplitude of the response to the test flash alone was longer in the patients than healthy control subjects. ISI indicates interstimulus interval; mtDNA, mitochondrial DNA.

a scotopic stimulus often used in routine clinical testing,<sup>41</sup> would have detected abnormal retinal function in only 2 of our patients in addition to those with congenital retinal blindness. Indeed, ERG evaluations that have used a limited number of stimulus conditions have not disclosed retinal dysfunction in patients with supposed mitochondrial disorders.<sup>42-44</sup> In the clinical context of multisystem involvement (Table 1), the pattern of ERG results summarized in Figure 2 leads one to include mitochondrial disorders in the differential diagnosis. This pattern contrasts with that found in some retinal degenerative disorders that begin in the outer segment and have early loss of b-wave amplitude rather than loss of sensitivity.<sup>45</sup>

In this sample, 3 (14%) of 22 patients initially had been seen as infants with visual impairment and attenuated ERG responses consistent with a clinical diagnosis of Leber congenital amaurosis, that is, congenital retinal blindness. Because of developmental delays and associated neurologic complaints, systemic workup was pursued and led to the findings of deficiencies in the mitochondrial enzyme complexes. Although mitochondrial disorders may not be a common cause of congenital retinal blindness, these 3 patients indicate that such disorders should be considered if congenital retinal blindness is associated with systemic abnormalities.

In 5 of the 22 patients, no rod-mediated dysfunction was detected. Two had visual deficits because of optic atrophy, but no mutations associated with Leber hereditary optic neuropathy. In the absence of demonstrated mutations of mtDNA, heteroplasmy<sup>46</sup> does not explain sparing of retinal function in these patients. The other 3 were among the youngest tested. There is some concern that they may, as time goes by, develop retinal dysfunction. Although, in this small cross-sectional study, the parameters of retinal function did not

worsen significantly with increasing age, the progressive course of our patient and others with Kearns-Sayre syndrome is a reminder of the potentially progressive involvement of the retina in mitochondrial disorders. Accordingly, we recommend that the retinal and visual function of patients with mitochondrial disorders be monitored.

Submitted for publication October 2, 2001; final revision received March 19, 2002; accepted April 24, 2002.

This study was supported in part by grant EY 10597 from the National Eye Institute, National Institutes of Health, Bethesda, Md.

Corresponding author and reprints: Anne B. Fulton, MD, Department of Ophthalmology, Children's Hospital Boston, 300 Longwood Ave, Boston, MA 02115 (e-mail: anne.fulton@tch.harvard.edu).

## REFERENCES

- Shoffner JM. Oxidative phosphorylation diseases. In: Scriver CR, Beaudet AL, Sly WS, Valle D, eds. *The Metabolic and Molecular Bases of Inherited Disease*. New York, NY: McGraw Hill Co; 2001:2367-2423.
- Rahman S, Schapira AHV. Mitochondrial myopathy: clinical features, molecular genetics, investigation and management. In: Schapira AHV, Griggs RC, eds. *Muscle Disease: Blue Books of Practical Neurology*. Boston, Mass: Butterworth-Heinemann; 1999:117-223.
- Steinberg R. Monitoring communications between photoreceptors and pigment epithelial cells: effects of "mild" systemic hypoxia. *Invest Ophthalmol Vis Sci*. 1987;28:1888-1904.
- Futterman S. Metabolism and photochemistry in the retina. In: Moses R, ed. *Adler's Physiology of the Eye*. St Louis, Mo: CV Mosby Co; 1975:406-419.
- Ames A III, Li Y-Y, Heher EC, Kimble CR. Energy metabolism of rabbit retina as related to function: high cost of Na<sup>+</sup> transport. *J Neurosci*. 1992;12:840-853.
- Young RW. Visual cells and the concept of renewal. *Invest Ophthalmol Vis Sci*. 1976;15:700-725.
- Pugh EN Jr, Lamb TD. Amplification and kinetics of the activation steps in phototransduction. *Biochim Biophys Acta*. 1993;1141:111-149.

8. Sjostrand F. The ultrastructure of the inner segments of the retinal rods of the guinea pig eye as revealed by electron microscopy. *J Cell Comp Physiol.* 1953; 42:45-70.
9. Wolbarsht M, George G, Shearin WA Jr, Kylstra J, Landers M III. Retinopathy of prematurity: a new look at an old disease. *Ophthalmic Surg.* 1983;14:919-924.
10. Runge P, Calver D, Marshall J, Taylor D. Histopathology of mitochondrial cytopathy and the Laurence-Moon-Biedl syndrome. *Br J Ophthalmol.* 1986;70: 782-796.
11. Phillips PH, Newman NJ. Mitochondrial diseases in pediatric ophthalmology. *J AAPOS.* 1997;1:115-122.
12. Ota Y, Miyake Y, Awaya S, Kumagai T, Tanaka M, Ozawa T. Early retinal involvement in mitochondrial myopathy with mitochondrial DNA deletion. *Retina.* 1994; 14:270-276.
13. Mullie MA, Harding AE, Petty RKH, Ikeda H, Morgan-Hughes JA, Sanders MD. The retinal manifestations of mitochondrial myopathy: a study of 22 cases. *Arch Ophthalmol.* 1985;103:1825-1830.
14. Ortiz RG, Newman NJ, Shoffner JM, Kaufman AE, Koontz DA, Wallace DC. Variable retinal and neurologic manifestations in patients harboring the mitochondrial DNA 8993 mutation. *Arch Ophthalmol.* 1993;111:1525-1530.
15. Newman NJ, Wallace DC. Mitochondria and Leber's hereditary optic atrophy. *Am J Ophthalmol.* 1990;109:726-730.
16. Dagi LR, Leys MJ, Hansen RM, Fulton AB. Hyperopia in complicated Leber's congenital amaurosis. *Arch Ophthalmol.* 1990;108:709-712.
17. Zheng XX, Shoffner JM, Voljavec AS, Wallace DC. Evaluation of procedures for assaying oxidative phosphorylation enzyme activities in mitochondrial myopathy muscle biopsies. *Biochim Biophys Acta.* 1990;1019:1-10.
18. Wallace DC, Zheng X, Lott MT, et al. Familial mitochondrial encephalomyopathy (MERRF): genetic, pathophysiological and biochemical characterization of a mitochondrial DNA disease. *Cell.* 1988;55:601-610.
19. Wongpichedchai S, Hansen RM, Koka B, Gudas VM, Fulton AB. Effects of halothane on children's electroretinograms. *Ophthalmology.* 1992;99:1309-1312.
20. Fulton AB, Hansen RM. The development of scotopic sensitivity. *Invest Ophthalmol Vis Sci.* 2000;41:1588-1596.
21. Hood DC, Birch DG. Rod phototransduction in retinitis pigmentosa: estimation and interpretation of parameters derived from the rod a-wave. *Invest Ophthalmol Vis Sci.* 1994;35:2948-2961.
22. Lamb TD, Pugh EN Jr. A quantitative account of the activation steps involved in phototransduction in amphibian photoreceptors. *J Physiol.* 1992;449:719-758.
23. Kraft TW, Schneeweis DM, Schnapf JL. Visual transduction in human rod photoreceptors. *J Physiol.* 1993;464:747-765.
24. Lyubarsky AL, Pugh EN Jr. Recovery phase of the murine rod photoreponse reconstructed from electroretinographic recordings. *J Neurosci.* 1996;16:563-571.
25. Birch DG, Hood DC, Nusinowitz S, Pepperberg DR. Abnormal activation and inactivation mechanisms of rod transduction in patients with autosomal dominant retinitis pigmentosa and the pro-23-his mutation. *Invest Ophthalmol Vis Sci.* 1995;36:1603-1614.
26. Pepperberg DR, Cornwall MC, Kahlert M, et al. Light-dependent delay in the fall-in phase of the retinal rod photoreponse. *Vis Neurosci.* 1992;8:9-18.
27. Pepperberg DR, Birch DG, Hofmann KP, Hood DC. Recovery kinetics of human rod phototransduction inferred from the two-branched a-wave saturation function. *J Opt Soc Am A Opt Image Sci Vis.* 1996;13:586-600.
28. Pepperberg DR, Birch DG, Hood DC. Photoresponse of human rods in vivo derived from paired flash electroretinograms. *Vis Neurosci.* 1997;14:73-82.
29. Peachey NS, Alexander KR, Fishman GA. The luminance-response function of the dark-adapted human electroretinogram. *Vision Res.* 1989;29:263-270.
30. Granit R. The components of the retinal action potential in mammals and their relation to the discharge in the optic nerve. *J Physiol.* 1933;77:207-239.
31. Granit R. The components of the vertebrate electroretinogram. In: *Sensory Mechanisms of the Retina.* London, England: Hafner Publishing Co; 1963:38-68.
32. Hood DC, Birch DG. A computational model of the amplitude and implicit time of the b-wave of the human ERG. *Vis Neurosci.* 1992;8:107-126.
33. Hood D, Birch D. Beta wave of the scotopic (rod) electroretinogram as a measure of the activity of human on-bipolar cells. *J Opt Soc Am A Opt Image Sci Vis.* 1996;13:623-633.
34. Aleman T, LaVail MM, Montemayor R, et al. Augmented rod bipolar cell function in partial receptor loss: an ERG study in P23H rhodopsin transgenic and aging normal rats. *Vis Res.* 2001;41:2779-2797.
35. Bush RA, Sieving PA. A proximal retinal component in the primate photopic ERG a-wave. *Invest Ophthalmol Vis Sci.* 1994;35:635-645.
36. Wurziger K, Lichtenberger T, Hanitzsch R. On-bipolar cells and depolarising third-order neurons as the origin of the ERG-b-wave in the RCS rat. *Vision Res.* 2001;41:1091-1101.
37. Robson J, Frishman L. Response linearity and kinetics of the cat retina: the bipolar cell component of the dark-adapted electroretinogram. *Vis Neurosci.* 1995; 12:837-850.
38. Robson JG, Frishman LJ. Photoreceptor and bipolar cell contributions to the cat electroretinogram: a kinetic model for the early part of the flash response. *J Opt Soc Am A Opt Image Sci Vis.* 1996;13:613-622.
39. Whitmore GA. Prediction limits for a univariate normal observation. *Am Stat.* 1986; 40:141-143.
40. Winkler B, Dang L, Malinoski C, Easter SJ. An assessment of rat photoreceptor sensitivity to mitochondrial blockade. *Invest Ophthalmol Vis Sci.* 1997;38:1569-1577.
41. Marmor MF, Zrenner E. Standard for clinical electroretinography. *Doc Ophthalmol.* 1995;89:199-210.
42. Ambrosio G, De Marco R, Loffredo L, Magli A. Visual dysfunction in patients with mitochondrial myopathies, I: electrophysiologic impairments. *Doc Ophthalmol.* 1995;89:211-218.
43. Berdjis H, Heider W, Demisch K. ERG and VEP in chronic progressive external ophthalmoplegia (CPEO). *Doc Ophthalmol.* 1985;60:427-434.
44. Harden A, Pampiglione G, Battaglia A. "Mitochondrial myopathy" or mitochondrial disease? EEG, ERG, VEP studies in 13 children. *J Neurol Neurosurg Psychiatry.* 1982;45:627-632.
45. Birch DG, Fish GE. Rod ERGs in retinitis pigmentosa and cone-rod degeneration. *Invest Ophthalmol Vis Sci.* 1987;28:140-150.
46. Shoffner JM, Wallace DC. Oxidative phosphorylation diseases: disorders of two genomes. *Adv Hum Genet.* 1990;19:267-330.

### CME Announcement

#### CME Hiatus: July Through December 2002

CME from *JAMA/Archives* will be suspended between July and December 2002. Beginning in early 2003, we will offer a new *online* CME program that will provide many enhancements:

- Article-specific questions
- Hypertext links from questions to the relevant content
- Online CME questionnaire
- Printable CME certificates and ability to access total CME credits

We apologize for the interruption in CME and hope that you will enjoy the improved online features that will be available in early 2003.